Fluid structure from density-functional theory

Matthias Schmidt
Institut für Theoretische Physik II, Heinrich-Heine-Universität Düsseldorf, Universitätsstraße 1, D-40225 Düsseldorf, Germany
(Received 11 May 2000)

We treat various common fluid models, like the inverse-power, Asakura-Oosawa, and Lennard-Jones potentials, within the soft fundamental measure theory (SFMT). We show that this recently proposed density-functional approach is able to predict the pair correlations in the fluid phase reliably compared to computer simulations. Explicit expressions for certain quantities of SFMT are given, namely, for the weight functions and the fundamental measures. These technical tools permit practical calculations for a large class of inhomogeneous systems.

PACS number(s): 64.10.+h, 61.20.Gy

I. INTRODUCTION

It is desirable that approximative density functionals [1] be simple. Simple theories are comprehensible and useful. Comprehensibility is desirable, because one can learn easily about the physics of the system. A theory is useful, of course, if it can be applied with small (or at least moderate) effort to an actual problem. The goal of theorists is to construct such simple theories, which despite their simplicity give excellent (or at least reasonable) results.

Among the many ways to construct density-functional theories (DFT's) the fundamental measure theory (FMT) is special, as it is able to predict the structure of the homogeneous bulk fluid state rather than needing it as an input. Following Rosenfeld's pioneering work for hard spheres [2], improved hard sphere functionals have been obtained [3–5] that are capable of describing inhomogeneous situations like, e.g., a solid [6,7,5] or depletion potentials in mixtures [8,9] excellently. For quite some time the FMT for hard sphere mixtures played a monolithic role, as its structure was (and still is) quite different from other DFTs. Heavily relying on insights in the analytic Percus-Yevick solution, scaled-particle theory, and integral geometry, it seemed, not only at first glance, that FMT works only for the special system of hard spheres. However, there have been numerous attempts to broaden the range of models covered by the theory, like the proposal of an extension to general hard convex bodies [10]. The FMT has been generalized to the more tractable system of hard parallel cubes [11–13].

It has turned out that the correct dimensional crossover [3,4] from three dimensions (3D) to lower ones, is an essential test for a DFT. One may even start from 0D situations of extreme confinement and construct 3D functionals systematically [14,5] using the idea of ''functional interpolation'' [5] between dimensions.

Surprisingly, the FMT machinery generates the thermodynamics, i.e., free energy, from the very basic situation of a cavity that has the size of one particle. For hard spheres the occupation number is zero or 1, and one can calculate the excess free energy exactly [3,4]. Applying this method to penetrable spheres, i.e., particles that may overlap at a finite energy cost, one obtains a reasonable approximation to the exact density functional of this system [15]. Concerning mixtures, recently a FMT for a nonadditive model colloid-polymer mixture was found [16]. However, in all these systems, the interactions are still step functions. This is a great simplification, as integral geometry can be fully exploited, essentially unchanged to the hard sphere case.

Among the attempts to treat soft interactions [17–19], the so-called soft fundamental measure theory (SFMT) [18,19] is also built on well-defined limiting cases, where the behavior of the exact free energy functional is known. These cases are the virial expansion and the 0D limit. However, two or three cavities, which are exact in hard sphere FMT, are not exact in SFMT. Nevertheless the application to the effective logarithmic interaction in star polymer solutions yields excellent results for the structure and the phase diagram [20]. Concerning its ease of use, however, the SFMT has the drawback that its weight functions are related to the Mayer function in a nontrivial way. This relation, the so-called deconvolution equation, is an integro-differential equation of second order in the unknown function. As will be discussed below, straightforward attempts to solve the deconvolution numerically are cumbersome; one encounters an inverse problem.

The aim of the present work is to give an explicit solution to the deconvolution equation. The availability of this solution allows the application of SFMT to a large class of statistical systems. Here we calculate the pair distribution functions in the bulk liquid for a variety of common models and find good agreement with simulation results.

In Sec. II the SFMT density functional is presented. The solution of the deconvolution equation is given in Sec. III. Examples for fluid structure are considered in Sec. V. Remarks are summarized in Sec. VI.

II. A DENSITY FUNCTIONAL

Within SFMT the excess free energy is approximated as

$$F^{\mathrm{exc}}(T,[\rho(\mathbf{r})])=k_{\mathrm{B}}T\int d\mathbf{x}\Phi(\{n_{\alpha}(T,\mathbf{x})\}), \qquad (1)$$

where T is the temperature, and k_{B} is Boltzmann's constant. The weighted densities n_{α} are obtained by convolutions of the weight functions with the one-body density profile $\rho(\mathbf{r})$,

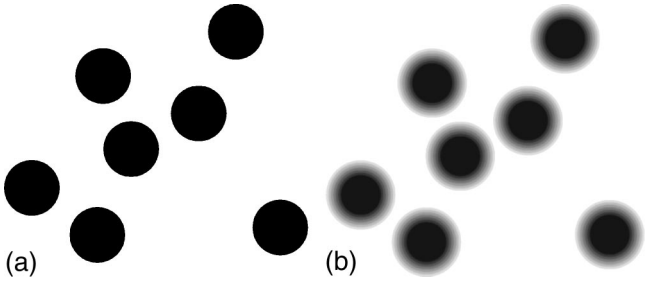

FIG. 1. Visualization of the weight functions describing single particles. (a) Hard spheres, (b) soft spheres.

$$n_\alpha(T,\mathbf{x}) = \int d\mathbf{r}\rho(\mathbf{r}) w_\alpha(T,\mathbf{x}-\mathbf{r}), \tag{2}$$

where α labels the type of the weight function. In the following we assume that the pair potential diverges at the origin. Then the free energy density is given by $\Phi = \Phi_1 + \Phi_2 + \Phi_3$, with the contributions

$$\Phi_1 = -n_0 \ln(1-n_3), \tag{3}$$

$$\Phi_2 = (n_1 n_2 - \mathbf{n}_{v1}\cdot\mathbf{n}_{v2})/(1-n_3), \tag{4}$$

$$\Phi_3 = \frac{\frac{1}{3}n_2^3 - n_2 \mathbf{n}_{v2}\cdot\mathbf{n}_{v2} + \frac{3}{2}(\mathbf{n}_{v2}\hat{\mathbf{n}}_{m2}\mathbf{n}_{v2} - 3\det\hat{\mathbf{n}}_{m2})}{8\pi(1-n_3)^2}, \tag{5}$$

where the caret denotes a second-rank tensor, and det is the determinant. The introduction of tensorial weighted densities, first done for hard spheres [5], leads to superior results in inhomogeneous situations [20] compared to the vectorial form [3,4,18]. The bulk fluid free energy and direct correlation function $c(r)$ are unaffected.

III. THE WEIGHT FUNCTIONS

The weight functions are given by the hierarchy

$$w_2(r) = -\frac{\partial w_3(r)}{\partial r}, \tag{6}$$

$$\mathbf{w}_{v2}(\mathbf{r}) = w_2(r)\mathbf{r}/r, \tag{7}$$

$$\mathbf{w}_{m2}(\mathbf{r}) = w_2(r)(\mathbf{rr}/r^2 - \hat{\mathbf{1}}/3), \tag{8}$$

$$w_1(r) = w_2(r)/(4\pi r), \tag{9}$$

$$\mathbf{w}_{v1}(\mathbf{r}) = w_1(r)\mathbf{r}/r, \tag{10}$$

$$w_0(r) = w_1(r)/r, \tag{11}$$

where w_2, w_1, w_0 are scalar quantities; $\mathbf{w}_{v1}, \mathbf{w}_{v2}$ are vectors, and $\hat{\mathbf{w}}_{m2}$ is a traceless matrix (where $\mathbf{rr}$ is a dyadic product and $\hat{\mathbf{1}}$ is the identity matrix). Dimensional analysis shows that the weight functions w_α carry the dimension of length to the power of $\alpha - d$, where $d=3$ is the dimensionality of the physical space. The hierarchy of weights (6)–(11) is built to recover the FMT weight functions [2,5] in the hard sphere limit. See Fig. 1 for a sketch; hard spheres are represented by sharp objects, soft spheres are washed out.

The weight functions are related to the Mayer function $f = \exp[-V(r)/k_BT] - 1$, where $V(r)$ is the pair potential, by

$$-\tfrac{1}{2} f(r) = w_0 * w_3 + w_1 * w_2 - \mathbf{w}_{v1} * \mathbf{w}_{v2}, \tag{12}$$

where the three-dimensional convolution, denoted by *, also implies scalar products between vectors. More explicitly, using Eqs.(6)–(11), this can be written (in r space) as

$$1 - \exp[-\beta V(r)] = \frac{1}{2\pi}\left(-\frac{w_3'(r)}{r^2} * w_3(r) + \frac{w_3'(r)}{r} * w_3'(r) - \frac{w_3'(r)}{r^2}\mathbf{r} * \mathbf{r}\frac{w_3'(r)}{r}\right), \tag{13}$$

where the prime denotes differentiation with respect to the argument r, and $\beta = 1/k_BT$. This *deconvolution equation* has to be solved for the unknown function $w_3(r)$ once a pair potential $V(r)$ is prescribed. The boundary conditions are $w_3(0)=1$ and $w_3(\infty)=0$ (see Appendix D). However, a direct numerical solution turns out to be impractical. Any uncertainties in w_3 become completely washed out under the convolution operation. Hence, iterative solution algorithms are unstable.

However, we can construct an explicit solution. It turns out that the Mayer function and the weight function w_2 have the simple relation

$$\frac{\partial f(r)}{\partial r} = \int_{-\infty}^{\infty} dr' w_2(r') w_2(r-r'), \tag{14}$$

where we formally set $w_2(r<0)=0$ to simplify the limits of integration. See Appendix A for the derivation of Eq. (14). In reciprocal space, we can write

$$\tilde{w}_2(k) = \pm\sqrt{ik\tilde{f}(k)}, \tag{15}$$

where the tilde denotes a one-dimensional Fourier transform, $\tilde{f}(k) = \int_{-\infty}^{\infty} dr f(r)\exp(ikr)$. Care has to be taken with the sign in Eq. (15). It may change depending on the value of k. As a physically meaningful prescription, we chose a continuous and differentiable function in k space.

A simple numerical algorithm works as follows. We start from $k=0$ and choose one of the signs, say the positive one. We proceed in small steps Δk. For each step, we check whether $ik\tilde{f}(k)$ attempts to cross the branch cut. If it does, we change the sign. Of course, more sophisticated root-finding algorithms can be used.

IV. FLUID FREE ENERGY

The free energy of the homogeneous fluid phase at a given density ρ and temperature T is

$$\frac{\beta F^{\text{exc}}}{V} = -n_0\ln(1-n_3) + \frac{n_1 n_2}{1-n_3} + \frac{n_2^3}{24\pi(1-n_3)^2} \tag{16}$$

The weighted densities become $n_\alpha = \xi_\alpha\rho$, where the fundamental measures ξ_α are defined as

$$\xi_\alpha = 4\pi \int_0^\infty dr r^2 w_\alpha(r). \tag{17}$$

The dimension of the fundamental measure ξ_α is the length scale to the power of α. For hard spheres, they are the volume $\xi_3 = 4\pi R^3/3$, surface area $\xi_2 = 4\pi R^2$, integral mean curvature $\xi_1 = R$, and Euler characteristic $\xi_0 = 1$. Using the soft weight functions one generalizes these quantities. The Euler characteristic is an integer, that is, roughly speaking, the number of connected portions minus the number of holes of a geometric shape. We find that the Euler characteristic is $\xi_0 = 1$, for any pair potential (see Appendixes B and D). This is consistent with the intuitive picture of soft spheres.

The ξ_α for $\alpha = 1,2,3$, however, need not be calculated directly from the weight functions. There is an easier way, as there are straightforward relations to moments of the Mayer function. We define

$$m_\alpha \equiv \int_0^\infty dr r^{\alpha-1} \{1 - \exp[-\beta V(r)]\} \tag{18}$$

as dimensional quantities. The index α gives the power of the length scale. Note that m_1 is the Barker-Henderson effective diameter [21]. Then the fundamental measures are related to the moments of the Mayer function via

$$\xi_0 = 1, \tag{19}$$

$$\xi_1 = m_1/2, \tag{20}$$

$$\xi_2 = 4\pi(m_2 - m_1^2/4), \tag{21}$$

$$\xi_3 = 2\pi(m_3 - m_2 m_1 + m_1^3/4). \tag{22}$$

This can be seen by a straightforward calculation (given in Appendix C).

V. APPLICATIONS

To test the theory we calculate pair distribution functions $g(r)$ for various fluid models. To this end we take the direct correlation function $c(r)$ given as a second functional derivative of the excess free energy, and use the Ornstein-Zernike relation in Fourier space to obtain the structure factor $S(k)$. A Fourier transform yields $g(r)$.

This procedure does not imply solving any equation numerically, except for the deconvolution Eq. (14). In particular, no density profile is calculated using the test-particle limit. Hence this is a severe test for the quality of the functional.

The results will be compared to simulations. We have carried out canonical Monte Carlo (MC) computer simulations with 512 particles and 10^5 MC moves per particle to collect data for $g(r)$. In all examples we have considered two reduced densities $\rho\sigma^3 = 0.1, 0.5$, where σ is the length scale appearing in the corresponding pair potential.

A. Error function model

We first consider a model potential that can be deconvolved analytically. It is a short-ranged potential with a steep repulsion given by the Mayer bond

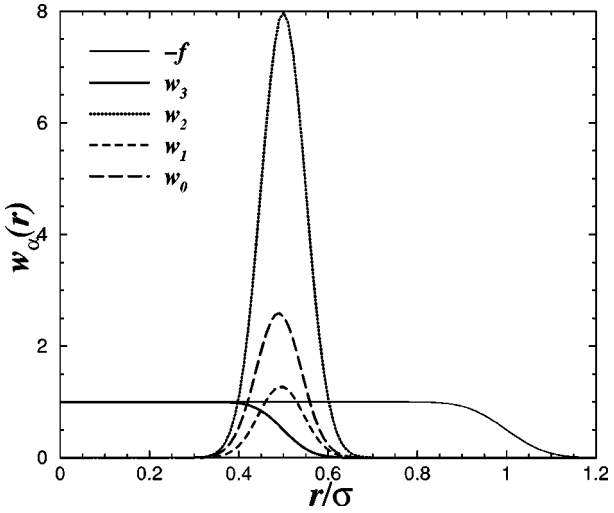

FIG. 2. Family of weight functions $w_\alpha(r)$ and the Mayer function $-f(r)$ for the erf model with $a/\sigma = 0.1$ as a function of the scaled distance r/σ.

$$f(r) = -\frac{1}{2}\left[1 - \mathrm{erf}\left(\frac{r-\sigma}{a}\right)\right], \tag{23}$$

where we use the convention $\mathrm{erf}(z) = (2/\sqrt{\pi})\int_0^z dt \exp(-t^2)$. We will assume that the scaled width a/σ is small, so that we can approximate $f(r=0) \approx -1$, as $\mathrm{erf}(r \to -\infty) = -1$ holds. As the Mayer bond equals an error function, we call this the erf model.

The derivative in real space is $f'(r) = \exp[-(r-\sigma)^2/a^2]/(a\sqrt{\pi})$. Its Fourier transform is also a Gaussian. Taking the square root, Eq. (15), Fourier transforming back, and integrating yields

$$w_3(r) = \frac{1}{2}\left[1 - \mathrm{erf}\left(\frac{r-(\sigma/2)}{a/\sqrt{2}}\right)\right]. \tag{24}$$

As expected, the length scale has changed from σ to $\sigma/2$. This means going from a description in terms of particle diameters to one in terms of particle radii. The shape of the two functions, however, is different. The width decreases only from a to $a/\sqrt{2}$. See Fig. 2 for a plot of the weight functions. In Fig. 3 results for the pair correlations are plotted for $a/\sigma = 0.1$. We find good agreement with the simulation result. The core condition, however, is not fulfilled exactly; small negative values for $g(r)$ are found for small distances. One could get rid of those using the test-particle limit.

B. Inverse-power potentials

We write the pair potential for ''soft spheres'' [22] as

$$V(r) = k_B T(\sigma/r)^p. \tag{25}$$

The moments of the Mayer function, Eq. (18), can be obtained analytically as

$$m_\alpha = \frac{\sigma^\alpha}{\alpha}\Gamma\left(1 - \frac{\alpha}{p}\right). \tag{26}$$

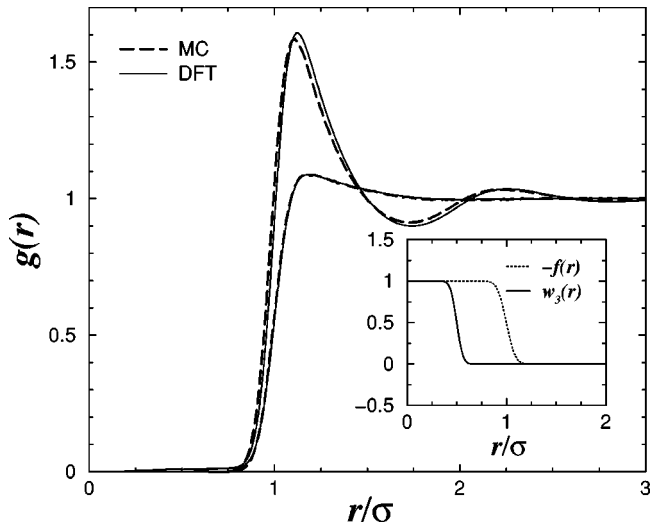

FIG. 3. Pair correlation function $g(r)$ obtained from density-functional theory (solid lines) compared to simulations (dashed) for the erf model with $a/\sigma=0.1$, $\rho\sigma^3=0.1,0.5$. The negative Mayer function $-f(r)$ and the weight function $w_3(r)$ are shown in the inset.

Using the relations between the m_α and the fundamental measures ξ_α, Eqs. (19) and (20)–(22), we get an analytical expression for the fluid free energy (16), similar, but not identical to the Barker-Henderson construction.

For small powers, $p\leqslant 3$, the fundamental measures diverge. Hence the theory cannot be applied as is. This reasoning is valid for any potential that has an inverse-power *tail*, i.e., decays as r^{-p} for $r\to\infty$. We will stay safely away from this problem and consider the exponent $p=12$. In Fig. 4 the pair correlations $g(r)$ are shown. The general agreement with MC data is good. For the moderate density $\rho\sigma^3=0.5$ the DFT result is shifted slightly to larger distances.

C. Asakura-Oosawa potential

The Asakura-Oosawa potential [23] is a prototype for depletion interactions. Considerable recent work is devoted to it; see, e.g., Refs. [24–26,16]. We write it as

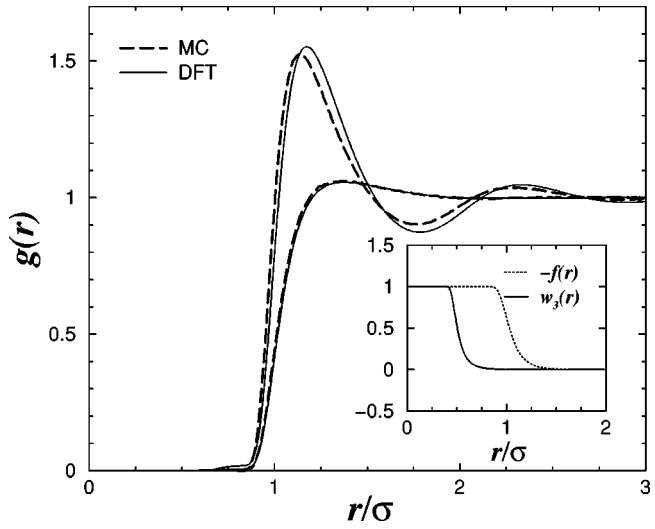

FIG. 4. Same as Fig. 3, but for the inverse-power potential with exponent $p=12$.

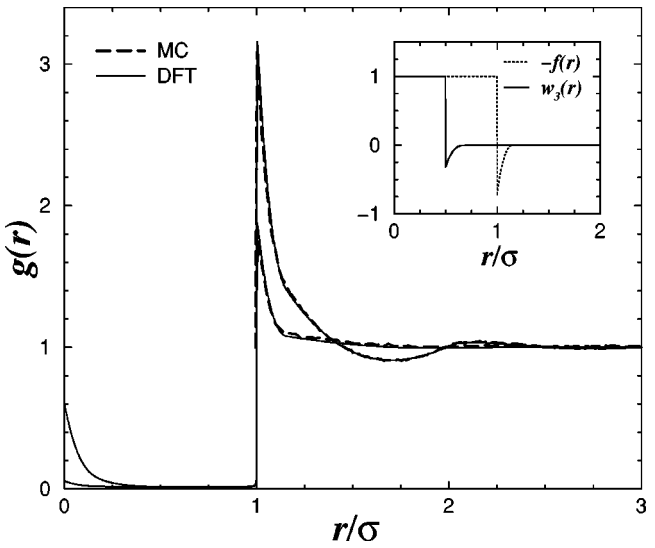

FIG. 5. Same as Fig. 3, but for the Asakura-Oosawa potential for $q=0.15,z=0.05$.

$$V(r)=\begin{cases}\infty, & r<\sigma\\ k_{\mathrm{B}}Tz\varphi(r), & \sigma<r<(1+q)\sigma\\ 0, & (1+q)\sigma<\infty,\end{cases}\tag{27}$$

$$\varphi(r)=-\left(\frac{1+q}{q}\right)^3\left(1-\frac{3r/\sigma}{2(1+q)}+\frac{(r/\sigma)^3}{2(1+q)^3}\right),\tag{28}$$

where the attraction is ruled by the (reduced) range q and the (reduced) strength z.

We show results for the state point $q=0.15,z=0.05$ in Fig. 5. The pair distributions $g(r)$ are remarkably good. The strong peak at contact as well as the second one are captured correctly. The core condition, however, is violated. A cusp near $r=0$ appears, where $g(r)$ has unphysical values that are forbidden by the hard core.

We emphasize that the deconvolution can be done for attractive potentials. The inset in Fig. 5 shows a comparison of $f(r)$ and the weight function $w_3(r)$. Apart from the halved length scale, both look similar, but $w_3(r)$ has a shallower negative well.

D. Lennard-Jones potential

The Lennard-Jones pair potential [22] is

$$V(r)=V_0[(\sigma/r)^{12}-(\sigma/r)^6].\tag{29}$$

Again the deconvolution is possible for this attractive potential. The pair correlations shown in Fig. 6 are slightly worse than in the above examples. For $\rho\sigma^3=0.5$ the height of the first peak is underestimated. The core is not reproduced, but has positive values.

The dotted line is the result for $\rho\sigma^3=0.5$ using a cutoff in the integration of the fundamental measures, Eq. (17). The upper limit of integration is reduced from infinity to the Wigner-Seitz radius $a=(4\pi\rho/3)^{-1/3}$. This procedure improves the result, but is somewhat heuristic and requires a better theoretical foundation.

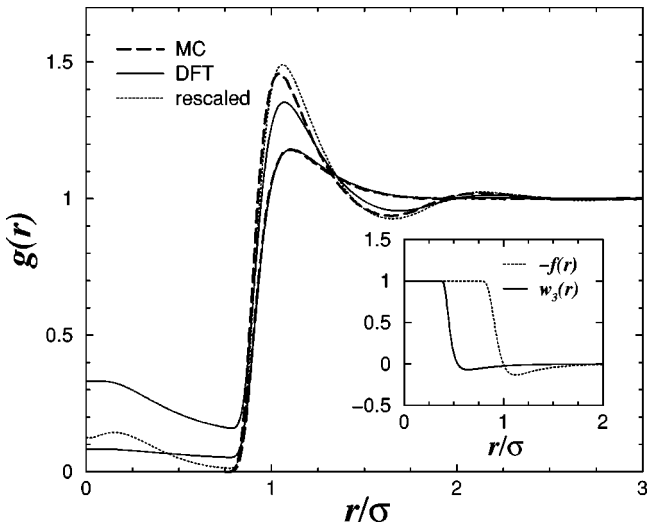

FIG. 6. Same as Fig. 3, but for the Lennard-Jones potential at $V_0/k_BT=0.5$.

VI. CONCLUSIONS

We have shown that soft fundamental measure theory is capable of predicting the fluid structure for repulsive as well as attractive interaction potentials. We have tested the pair correlations from the theory against computer simulation results at moderate density, moderate softness, and moderate attraction. We find good agreement, except for small artifacts inside the core.

We emphasize that the current approach is expected to work best for potentials that are still dominated by packing effects, i.e., are sufficiently short ranged. True long-ranged potentials like the Coulomb or inverse-power potential with small exponents cannot be tackled. Also, a possible attraction needs to be sufficiently weak and short ranged, as present in the example of the Asakura-Oosawa potential above, to be described correctly.

The utility of SFMT depends crucially on the accessibility of the functional form of the weight functions. In this work we give an explicit solution to the deconvolution equation that relates the Mayer bond to the weight functions. The solution requires only one-dimensional Fourier transforms and the handling of a root-finding problem in reciprocal space. Numerically, both operations are simple.

ACKNOWLEDGMENTS

I thank Roland Roth and Andreas Lang for useful comments.

APPENDIX A: DECONVOLUTION OF THE MAYER BOND

From the relation between the weights, Eq. (6), we obtain

$$w_3(r)=\int_r^\infty dr' w_2(r'), \tag{A1}$$

which can be turned into a convolution

$$w_3(r)=\int_0^\infty dr' w_2(r')\Theta(r'-r). \tag{A2}$$

Applying the hierarchy of weights Eqs. (6)–(11) to Eq. (A2) yields the relations

$$w_\alpha(r)=\int_0^\infty dr' w_2(r') h_{\alpha,r'}(r), \tag{A3}$$

where the $h_{\alpha,r'}(r)$ equal the hard sphere weight functions with radius r' and are given by $h_{3,r'}(r)=\Theta(r'-r)$, $h_{2,r'}(r)=\delta(r'-r), h_{1,r'}(r)=\delta(r'-r)/(4\pi r)$, $h_{0,r'}(r)=\delta(r'-r)/(4\pi r^2)$, $\mathbf{h}_{\mathrm{v2},r'}(r)=\delta(r'-r)\mathbf{r}/r$, $\mathbf{h}_{\mathrm{v1},r'}(r)=\delta(r'-r)\mathbf{r}/(4\pi r^2)$.

Next we insert Eq. (A3) into the deconvolution equation (12) to obtain

$$-\frac{1}{2}f(r)=\int_0^\infty dr' w_2(r')\int_0^\infty dr'' w_2(r'')K(r,r',r''), \tag{A4}$$

$$K(r,r',r'')=h_{3,r'}(r)*h_{0,r''}(r)+h_{2,r'}(r)*h_{1,r''}(r) -\mathbf{h}_{\mathrm{v2},r'}(r)*\mathbf{h}_{\mathrm{v1},r''}(r). \tag{A5}$$

We observe that the convolution kernel, Eq. (A5), is the well-known deconvolution of the hard sphere Mayer bond [2],

$$K(r,r',r'')=\frac{1}{2}\Theta(r'+r''-r). \tag{A6}$$

Inserting this into Eq. (A4) and differentiating gives

$$f'(r)=\int_0^\infty dr' w_2(r')\int_0^\infty dr'' w_2(r'')\,\delta(r'+r''-r), \tag{A7}$$

from which we obtain Eq. (14) by a straightforward integration over r''.

APPENDIX B: FUNDAMENTAL MEASURES AND THE VOLUME WEIGHT

Integrating Eq. (17) by parts yields the useful relations

$$\xi_3=4\pi\int_0^\infty dr\, r^2 w_3(r), \tag{B1}$$

$$\xi_2=8\pi\int_0^\infty dr\, r w_3(r), \tag{B2}$$

$$\xi_1=\int_0^\infty dr\, w_3(r), \tag{B3}$$

$$\xi_0=w_3(0)-w_3(\infty)=1. \tag{B4}$$

See Appendix D for the justification of the last equality sign.

APPENDIX C: FUNDAMENTAL MEASURES AND THE MAYER FUNCTION

Integrating the definition of the moments of the Mayer function, Eq. (18), by parts yields

$$m_\alpha = \alpha^{-1} \int_0^\infty dr\, r^\alpha f'(r), \tag{C1}$$

where the boundary terms vanish, as we assume $f(0) = -1$, $f(\infty) = 0$. Expressing the derivative of the Mayer bond through the convolution of weights (14) gives

$$m_\alpha = \alpha^{-1} \int_0^\infty dr\, r^\alpha \int_0^\infty dr' w_2(r') w_2(r - r'). \tag{C2}$$

Changing integration variables, $r'' = r - r'$, gives

$$\alpha m_\alpha = \int_0^\infty dr' \int_0^\infty dr''(r' + r'')^\alpha w_2(r') w_2(r'') \tag{C3}$$

$$= \sum_{i=0}^{\alpha} \binom{\alpha}{i} \int_0^\infty dr' (r')^i w_2(r') \int_0^\infty dr''(r'')^{\alpha - i} w_2(r''). \tag{C4}$$

Explicitly treating the cases $\alpha = 1,2,3$ yields Eqs. (20), (21), and (22), respectively.

APPENDIX D: BOUNDARY CONDITIONS OF THE VOLUME WEIGHT

The requirement that the DFT fulfils the 0D limit yields boundary conditions for the volume weight function w_3. Consider a 0D density distribution $\rho(\mathbf{r}) = \eta \delta(\mathbf{r})$. The weighted densities are $n_\alpha(\mathbf{r}) = \eta w_\alpha(\mathbf{r})$. Symmetry between the weight functions leads to $\Phi_2 = \Phi_3 = 0$. The remaining term Φ_1 gives

$$\beta F^{\mathrm{exc}}[\eta \delta(\mathbf{r})] = \int_0^\infty dr\, \eta w_3'(r) \ln[1 - \eta w_3(r)], \tag{D1}$$

where we have used $w_0(r) = -(4\pi r^2)^{-1} \partial w_3(r)/\partial r$ [see Eqs. (6)–(11)]. We change integration variables to $u = \eta w_3$ and obtain

$$\beta F^{\mathrm{exc}}[\eta \delta(\mathbf{r})] = \int_{u_0}^{u_\infty} du \ln(1 - u), \tag{D2}$$

where the limits are $u_0 = \eta w_3(0)$ and $u_\infty = \eta w_3(\infty)$. If we assume that the boundary conditions are $w_3(0) = 1$ and $w_3(\infty) = 0$, then the integral gives the exact 0D excess free energy [3,4,18], which is $\beta F_{0\mathrm{D}} = \eta + (1 - \eta)\ln(1 - \eta)$.

[1] R. Evans, in *Fundamentals of Inhomogeneous Fluids*, edited by D. Henderson (Wiley, New York, 1992), p. 85.
[2] Y. Rosenfeld, Phys. Rev. Lett. **63**, 980 (1989).
[3] Y. Rosenfeld, M. Schmidt, H. Löwen, and P. Tarazona, J. Phys.: Condens. Matter **8**, L577 (1996).
[4] Y. Rosenfeld, M. Schmidt, H. Löwen, and P. Tarazona, Phys. Rev. E **55**, 4245 (1997).
[5] P. Tarazona, Phys. Rev. Lett. **84**, 694 (2000).
[6] B. Groh and B. Mulder, Phys. Rev. E **61**, 3811 (2000).
[7] B. Groh, Phys. Rev. E **61**, 5218 (2000).
[8] R. Roth, B. Götzelmann, and S. Dietrich, Phys. Rev. Lett. **83**, 448 (1999).
[9] R. Roth, Ph.D. thesis, Bergische Universität-Gesamthochschule Wuppertal, 1999.
[10] Y. Rosenfeld, Phys. Rev. E **50**, R3318 (1994).
[11] J. A. Cuesta, Phys. Rev. Lett. **76**, 3742 (1996).
[12] J. A. Cuesta and Y. Martinez-Raton, Phys. Rev. Lett. **78**, 3681 (1997).
[13] J. A. Cuesta and Y. Martinez-Raton, J. Chem. Phys. **107**, 6379 (1997).
[14] P. Tarazona and Y. Rosenfeld, Phys. Rev. E **55**, R4873 (1997).
[15] M. Schmidt, J. Phys.: Condens. Matter **11**, 10163 (1999).
[16] M. Schmidt, H. Löwen, J. M. Brader, and R. Evans, Phys. Rev. Lett. **85**, 1934 (2000).
[17] M. B. Sweatman, Ph.D. thesis, University of Bristol, 1995.
[18] M. Schmidt, Phys. Rev. E **60**, R6291 (1999).
[19] M. Schmidt, Phys. Rev. E **62**, 3799 (2000).
[20] B. Groh and M. Schmidt (unpublished).
[21] J. A. Barker and D. Henderson, J. Chem. Phys. **47**, 4714 (1967).
[22] J. P. Hansen and I. R. McDonald, *Theory of Simple Liquids*, 2nd ed. (Academic Press, London, 1986).
[23] S. Asakura and F. Oosawa, J. Chem. Phys. **22**, 1255 (1954).
[24] A. A. Louis, R. Finken, and J. Hansen, Europhys. Lett. **46**, 741 (1999).
[25] M. Dijkstra, J. M. Brader, and R. Evans, J. Phys.: Condens. Matter **11**, 10079 (1999).
[26] J. M. Brader and R. Evans, Europhys. Lett. **49**, 678 (2000).